Consequences of parameterization choice on eclipsing binary light curve solutions

J. Korth[1], A. Moharana[2], M. Pešta[3], D.R. Czavalinga[4] and K.E. Conroy[5]

[1] *Rheinisches Institut für Umweltforschung, Abteilung Planetenforschung an der Universität zu Köln, Universität zu Köln, Aachenerstrae 209, 50931 Köln, (E-mail: judithkorth@gmail.com)*

[2] *Nicolaus Copernicus Astronomical Center, Polish Academy of Sciences, ul. Rabiańska 8, 87-100 Toruń, Poland, (E-mail: ayushm@ncac.torun.pl)*

[3] *Institute of Theoretical Physics, Charles University, V Holešovičkách 2, 180 00 Praha 8, Czech Republic, (E-mail: pestamilan@gmail.com)*

[4] *Institute of Physics, University of Szeged, 6720 Szeged, Hungary, (E-mail: czdonat@titan.physx.u-szeged.hu)*

[5] *Department of Astrophysics and Planetary Science, Villanova University, 800 East Lancaster Avenue, Villanova, PA 19085, USA*

Abstract. Eclipsing Binaries (EBs) are known to be the source of most accurate stellar parameters, which are important for testing theories of stellar evolution. With improved quality and quantity of observations using space telescopes like *TESS*, there is an urgent need for accuracy in modeling to obtain precise parameters. We use the soon to be released `PHOEBE 2.3` EB modeling package to test the robustness and accuracy of parameters and their dependency on choice of parameters for optimization.

Key words: Stars: binaries: eclipsing – stars: fundamental parameters – methods: numerical

1. Introduction

It is well known that eclipsing binaries (EBs) provide highly accurate observations of stellar parameters, which is important for testing theories of star evolution. Thanks to the increasingly more precise photometry of the past and recent space missions (e.g. *Kepler* (Borucki, 2016) and the Transiting Exoplanet Survey Satellite (*TESS*;Ricker et al., 2014)), it is now possible to observe and study EBs in details never seen before (e.g. reflection from the companion, lensing, or Doppler beaming). To understand the observations, one needs to employ

models capable of making predictions with sufficient precision, so that it is possible to compare the observations with predicted theoretical values. A popular example of such software is PHOEBE (Prša et al., 2016; Horvat et al., 2018; Jones et al., 2020), a robust Python package for modeling of EB systems. The latest release provides users with control over a large number of orbital and physical parameters, which allows them to generate synthetic light curves and radial velocities of the binary system. One can also take advantage of various built-in or imported solvers (e.g. emcee) and optimizers (e.g. Nelder-Mead) to solve the inverse problem—for a comprehensive introduction to the inverse problem using PHOEBE see Conroy et al. (2020).

For the purpose of this paper, we use the soon to be released version 2.3 of PHOEBE to try and reproduce the results from the article by Maxted et al. (2020), which examines a number of various methods to accurately estimate the masses and radii for the stars in the binary system AI Phoenicis (AI Phe). This system, which contains two well-separated, sharp-lined stars of comparable luminosity, was first identified as an EB by Strohmeier (1972). It is an excellent target for model testing as it is relatively bright ($V = 8.6\,\mathrm{mag}$), has a long orbital period ($P \approx 24.59\,\mathrm{days}$), and does not show any distinct spots nor flares associated with increased magnetic activity of the components (e.g., Kirkby-Kent et al., 2016; Maxted et al., 2020).

To compare the results by Maxted et al. (2020), we first carried out a number of runs with varying underlying physical models, free parameters, and their initial values (see Section 2). This further motivated us to design a controlled experiment in order to systematically analyze the effect of parameterization choice on the final light curve resulting from the model (Section 3). Finally, in Section 4, we compare our results from the controlled experiment with the Maxted et al. (2020) values, and we discuss our findings regarding the precision of the employed model.

2. Observations and Modeling Set-up

The photometric data of AI Phe used in the subsequent analyses were obtained under the *TESS* Guest Investigator Program (G011130, P.I. Maxted; G011083, P.I. Helminiak; G011154, P.I. Pra) during Sector 2 of the *TESS* mission observed in the 2-min cadence mode (TIC 102069549). The Sector was observed for 27 days from 2458354.113259 BJD to 2458381.517643 BJD (covering both the primary and secondary eclipse), and the data were reduced by the *TESS* data processing pipeline developed by the Science Processing Operations Center (SPOC; Jenkins et al., 2016). In our analyses, we used the Pre-search Data Conditioning Simple Aperture Photometry (PDCSAP) light curve, which was additionally detrended by fitting a chain of 5th order Legendre polynomials (Maxted et al., 2020, Section 2.6).

To get a sense of the effect of parameterization on the resulting values, we independently solved the inverse problem for AI Phe by using a separate model with its own set of free parameters and approximation of physical phenomena (e.g. limb-darkening law, reflection, etc.). Following the approach from Maxted et al. (2020), we initialized the parameters of the models with their estimates from Kirkby-Kent et al. (2016), which are summarized in Table 1.

Table 1. A list of the parameters of the binary system AI Phe that were adopted from Kirkby-Kent et al. (2016).

Parameters	Values
P (days)	24.592483
q	1.0417
e	0.1821
$\omega(^o$)	110.73
$i(^o$)	88.502
M_1 (($M_\odot$)	1.1973
M_2 (($M_\odot$)	1.2473
R_1 (($R_\odot$))	1.835
R_2 (($R_\odot$))	2.912
T_1 (K)	6310
T_2 (K)	5237.3

The initialized free parameters were used as input to the Nelder-Mead algorithm (Nelder & Mead, 1965) in order to refine the estimates. These estimates then served as a starting point for initial distributions (either Gaussian or uniform) of the free parameters entering the Markov Chain Monte Carlo (MCMC) algorithm implemented in the `emcee` solver (Foreman-Mackey et al., 2013), which we used to obtain posterior distributions of the relevant parameters. Furthermore, we used the following software: `Python` (Van Rossum & Drake, 2009), and the `Python` libraries `Matplotlib` (Hunter, 2007) and `numpy` (van der Walt et al., 2011).

Unfortunately, the individual runs did not yield satisfactory results as the obtained values showed a wide spread. Due to the different choices of parameterization and the large numbers of parameters, it was not possible to associate the observed variation with a specific parameter or a set of parameters. Therefore, we decided to design a controlled experiment, in which we defined a "nominal" run and then we examined the effect of altering the parameters one at a time. For more information see the following section.

3. Controlled Experiment

The "nominal" run (which we shall denote "Run A") served as a benchmark for all the other runs ("B" through "K"), which we systematically varied from Run A in a controlled fashion—that is, for each run, we altered one aspect of the "nominal" set-up and kept the rest unchanged. For the definitions of Runs B–K, see Table 2.

Table 2. A list of the individual runs and their differences from the "nominal" run.

Run	Description
A	The "nominal" run
B	Logarithmic limb darkening law
C	Sample/interpolate in phase-space
D	Marginalization over albedos
E	Marginalization over gravity darkening parameters
F	Marginalization over gravity darkening parameters from Claret & Bloemen (2011)
G	Marginalization over noise nuissance parameter
H	Marginalization over parameters q and a using radial velocities posteriors from Gallenne et al. (2019) on q and $a \sin i$
I	Meshes on binary surfaces to estimate L_{pb}
J	*TESS* light curve without detrending (PDCSAP)
K	Masking the out-of-eclipse points

Run A uses the binary star model ELLC (for more information see Maxted, 2016) with the quadratic limb-darkening law in the "lookup" mode (automatic querying of coefficients from tables based on mean stellar values), and uses the Stefan-Boltzmann approximation in the determination of the passband luminosity, L_{pb}, which is needed to scale the fluxes and estimate the surface-brightness ratio. Similar to our initial test runs, we initialized the parameters with values from Kirkby-Kent et al. (2016), and then used the Nelder-Mead algorithm to refine the estimates. After that, we used the `emcee` solver to sample over the radii, R_1 and R_2, (for the primary and secondary component), the eccentricity, e, along with the argument of pericenter, ω_0, (parameterized as $e \sin \omega_0$ and $e \cos \omega_0$), the time of the primary eclipse, T_0, the third light, l_3, L_{pb}, the ratio of the effective temperature of the secondary and primary component, $T_{\mathrm{secondary}}/T_{\mathrm{primary}}$, and the orbital inclination, i, to get an estimate for their uncertainties. We present the obtained results in Fig. 1.
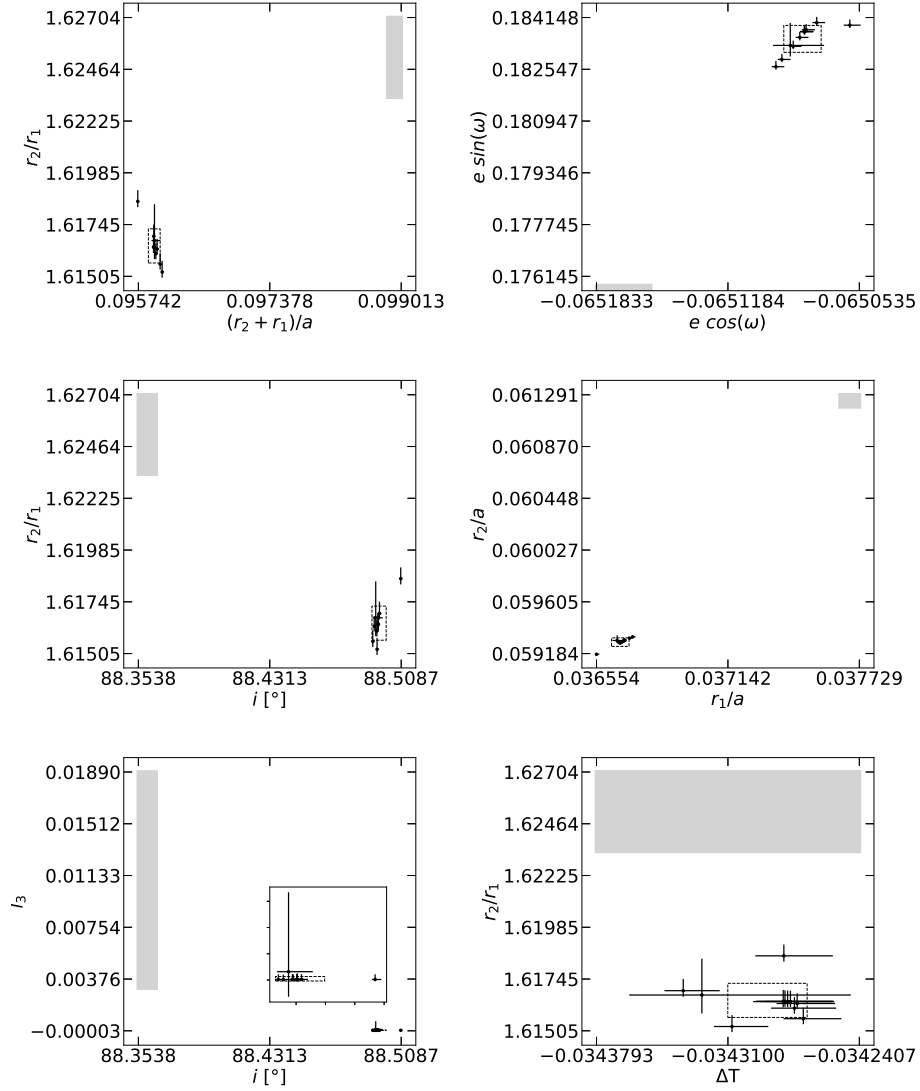
Figure 1. A comparison between the parameters resulting from Runs A–K and those obtained by Maxted et al. (2020). The filled rectangle represents the 1-σ spread around the average of the runs from the Maxted et al. paper (see Table 3), while the dotted box shows the same for our controlled runs. The inner box in the l_3 vs i plot represents a zoomed-in view on the parameter distribution.

4. Discussion of Results

Analysis of Runs A–K shows a rather limited spread of the obtained values, with the individual parameters lying within each other's uncertainties (see Fig. 1). Seeing that the parameters have a fairly small effect on the final results, this implies that the high variation of our initial runs was most likely not caused by any specific parameter but rather by a combined effect of various parameterization choices. That said, it is still clear that the choices made in Table 2 do influence the final results.

As for the runs presented in Maxted et al. (2020), each of them employs a distinct combination of the underlying physical model, optimization method and parameterization (see Table 3). In principle, to properly compare our results with those obtained by Maxted et al. (2020), the initial set-ups should also be compared so that the effect of initial configuration choice can be distinguished from other effects. Although we compare our results with all the runs listed in Table 3 (see Fig. 1), we shall inspect in detail only the initial set-ups for Runs A and S by Maxted, as they utilize the same physical binary model (`ellc`) and optimization method (`emcee`) as our runs. Our runs use a wrapper for mapping of `PHOEBE` parameterization onto `ellc`), and thus they minimize the effect of choice (there is still the freedom of parameterization) and can serve as a "benchmark" for our results. Moreover, Runs A and S by Maxted use essentially the same initial set-ups, therefore it suffices to examine only the former (which additionally corrects for instrumental systematic variations). To avoid confusion, we shall prefix the runs by Maxted et al. (2020) with "M-" (e.g. Run A by Maxted becomes Run M-A) in the rest of the section.

For the sake of simplicity, we shall compare the parameterization of Run M-A only with our "nominal" Run A, which is assumed to be representative of the other runs (for their definitions, see Table 2). In Table 4, we compare the free parameters entering the `emcee` algorithm in the two runs. Apart from working with mostly disjunct (but correlated) sets of free parameters, the runs also differ in the limb-darkening law (power-2 for Run M-A and quadratic for Run A) and the treatment of the stellar masses. Run A adopts the values $1.1973 \, \mathrm{M_\odot}$ and 1.0417 from Kirkby-Kent et al. (2016) for the mass of the primary component and the ratio of the masses of the secondary and primary component, respectively. In addition, the stellar masses are held constant at the Kirkby-Kent values as they have minimal effect on the light curve. In contrast, Run M-A uses the `emcee` posterior distributions of the free parameters together with observed radial velocities of the binary system to get an estimate for the masses. Finally, both runs hold the semi-major axis constant, with Run M-A assuming the value of $47.868 \, \mathrm{R_\odot}$ and Run A keeping it equal to $47.941 \, \mathrm{R_\odot}$.

Coming back to the general case, we expected our results to agree with those obtained by Maxted et al. (2020) within the reported uncertainties despite the

Table 3. An overview of the various runs analysed in the paper by Maxted et al. (2020). The table was adopted from page 6 of the mentioned paper.

Run	Investigator	Model	Optimization	Limb-darkening	Detrending	Notes
A	Maxted	`ellc`	`emcee`	power-2	`celerite`	
B	Helminiak	`JKTEPOB`	L-M	quadratic	sine+poly	Monte Carlo error estimated
C	Torres	EB	`emcee`	quadratic	spline	Quadratic l.d. coeffs. fixed
D	”	”	”	”	”	
E	Graczyk	WD2007	L-M	logarithmic	–	Fixed l.d. coefficients
F	Johnston	`PHOEBE 1.0`	`emcee`	square-root	–	
G	Pra	`PHOEBE 2.1`	MCMC	grid	legendre	
H	Orosz	ELC	DE-MCMC	logarithmic	polynomial	
I	Orosz	”	”	square-root	”	
J	Orosz	”	”	quadratic	”	
K	Southworth	`JKTEBOP`	L-M	quadratic	polynomial	
L	Southworth	`JKTEBOP`	L-M	cubic	polynomial	
S	Maxted	`ellc`	`emcee`	power-2	`celerite`	Same as Run A with SAP light curve

Table 4. A list of the free parameters entering the `emcee` algorithm in Runs M-A and A. The "Nelder-Mead" column marks the parameters which were optimized before running `emcee`, in order to speed-up the convergence of the posterior distributions.

Parameter	Description	Run M-A	Run A	
		emcee	Nelder-Mead	emcee
$e\cos\omega$			✓	✓
$e\sin\omega$			✓	✓
f	Flux scaling factor	✓		
f_c	$\sqrt{e}\cos\omega$	✓		
f_s	$\sqrt{e}\sin\omega$	✓		
$h_{1,\mathrm{F}}, h_{2,\mathrm{F}}$	Parameters of the power-2 limb darkening law for star 1	✓		
$h_{1,\mathrm{K}}, h_{2,\mathrm{K}}$	Parameters of the power-2 limb darkening law for star 2	✓		
i	Orbital inclination	✓	✓	✓
k	Ratio of the radii	✓		
l_3	Third light	✓		✓
L_{pb}	Passband luminosity			✓
r_{sum}	Sum of the fractional radii	✓		
R_1	Radius of the primary star		✓	✓
R_2	Radius of the secondary star		✓	✓
σ_f	Standard error per observation	✓		
S_{T}	Surface brightness ratio averaged over the stellar disks in the TESS band	✓		
T_0	Time of primary eclipse	✓	✓	✓
$T_{\mathrm{secondary}}/T_{\mathrm{primary}}$	Ratio of the effective temperatures		✓	✓

differences in the initial set-ups of the runs. However, Fig. 1 shows that this is not the case as none of the results from Runs AK lies in the 1-sigma spread of the Maxted et al. (2020) values. As to the reason behind this discrepancy, multiple explanations present themselves. First, due to time and computational

constraints, we stopped our `emcee` runs after appearing flat (converged to a single value) for about 1500 iterations compared to $\sim$10000 iterations for the runs in Maxted et al. (2020). Thus, there is a slight possibility that the runs might yet "jump" and converge to some other values. All of our runs, however, were treated consistently with each other, and still exhibit the influence of a number of decisions in the fitting process on the final results. Next, the mapping between the `PHOEBE` and `ellc` parameterizations includes several assumptions and approximations, which leads to residuals between the two forward models (see Fig. 2). This suggests that the offset between the two sets of results might be caused by not employing the native `PHOEBE` backend.
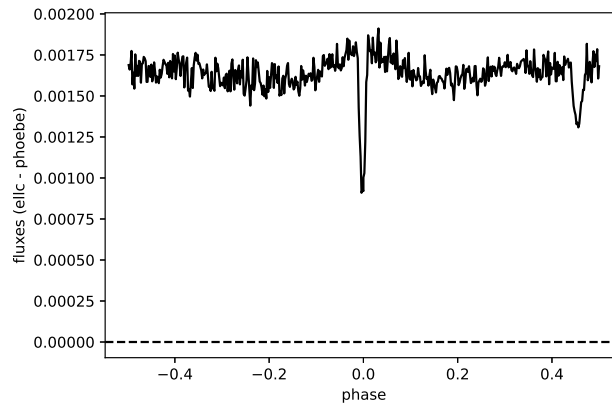

Figure 2. Residuals between the `ellc` and `PHOEBE` forward models for the nominal case. This shows the influence of the approximations in mapping between the parameterization of the different codes and likely explains the offset between the results from our controlled sample and those in Maxted et al. (2020).

5. Conclusions

In this work, we tried to fit the parameters of AI Phoenicis from the *TESS* light curve and to reproduce the values estimated by Maxted et al. (2020). First, we independently modeled the light curves with individual sets of free parameters and their approximations, e.g., difference between initialized parameters of binary masses, radius, effective temperatures of the stars, or model of limb darkening, reflections etc. Since our independent models did not lead to the same results for the system parameters of AI Phe, we designed a controlled experiment to systematically analyze the effect of the parameterization.

The parameters obtained from different runs were expected to be distributed in a parameter space as found in Maxted et al. (2020) but we find our results to be quite different in comparison to the accuracy that has been found before. We suspect the discrepancy may be reconciled by running `emcee` for substantially longer to allow further convergence and to switch to the native `PHOEBE` forward model to avoid the assumptions and approximations in the translation between parameterizations. Our results do, however, show the importance of several different choices in the fitting process on the final parameter values and their uncertainties.

Acknowledgements.

References

Borucki, W. J., KEPLER Mission: development and overview. 2016, *Reports on Progress in Physics*, **79**, 036901, DOI: 10.1088/0034-4885/79/3/036901

Claret, A. & Bloemen, S., Gravity and limb-darkening coefficients for the Kepler, CoRoT, Spitzer, uvby, UBVRIJHK, and Sloan photometric systems. 2011, *Astronomy and Astrophysics*, **529**, A75, DOI: 10.1051/0004-6361/201116451

Conroy, K. E., Kochoska, A., Hey, D., et al., Physics of Eclipsing Binaries. V. General Framework for Solving the Inverse Problem. 2020, *arXiv e-prints*, arXiv:2006.16951

Foreman-Mackey, D., Hogg, D. W., Lang, D., & Goodman, J., emcee: The MCMC Hammer. 2013, *Publications of the Astronomical Society of the Pacific*, **125**, 306, DOI: 10.1086/670067

Gallenne, A., Pietrzyński, G., Graczyk, D., et al., The Araucaria project: High-precision orbital parallax and masses of eclipsing binaries from infrared interferometry. 2019, *Astronomy and Astrophysics*, **632**, A31, DOI: 10.1051/0004-6361/201935837

Horvat, M., Conroy, K. E., Pablo, H., et al., Physics of Eclipsing Binaries. III. Spin–Orbit Misalignment. 2018, *The Astrophysical Journal Supplement Series*, **237**, 26, DOI: 10.3847/1538-4365/aacd0f

Hunter, J. D., Matplotlib: A 2D graphics environment. 2007, *Computing in Science & Engineering*, **9**, 90, DOI: 10.1109/MCSE.2007.55

Jenkins, J. M., Twicken, J. D., McCauliff, S., et al., The TESS science processing operations center. 2016, in Society of Photo-Optical Instrumentation Engineers (SPIE) Conference Series, Vol. **9913**, *Software and Cyberinfrastructure for Astronomy IV*, 99133E

Jones, D., Conroy, K. E., Horvat, M., et al., Physics of Eclipsing Binaries. IV. The Impact of Interstellar Extinction on the Light Curves of Eclipsing Binaries. 2020, *The Astrophysical Journal Supplement Series*, **247**, 63, DOI: 10.3847/1538-4365/ab7927

Kirkby-Kent, J. A., Maxted, P. F. L., Serenelli, A. M., et al., Absolute parameters for AI Phoenicis using WASP photometry. 2016, *Astronomy and Astrophysics*, **591**, A124, DOI: 10.1051/0004-6361/201628581

Maxted, P. F. L., ellc: A fast, flexible light curve model for detached eclipsing binary stars and transiting exoplanets. 2016, *Astronomy and Astrophysics*, **591**, A111, DOI: 10.1051/0004-6361/201628579

Maxted, P. F. L., Gaulme, P., Graczyk, D., et al., The TESS light curve of AI Phoenicis. 2020, *Monthly Notices of the RAS*, **498**, 332, DOI: 10.1093/mnras/staa1662

Nelder, J. A. & Mead, R., A Simplex Method for Function Minimization. 1965, *The Computer Journal*, **7**, 308, DOI: 10.1093/comjnl/7.4.308

Prša, A., Conroy, K. E., Horvat, M., et al., PHYSICS OF ECLIPSING BINARIES. II. TOWARD THE INCREASED MODEL FIDELITY. 2016, *The Astrophysical Journal Supplement Series*, **227**, 29, DOI: 10.3847/1538-4365/227/2/29

Ricker, G. R., Winn, J. N., Vanderspek, R., et al., Transiting Exoplanet Survey Satellite (TESS). 2014, in Society of Photo-Optical Instrumentation Engineers (SPIE) Conference Series, Vol. **9143**, *Space Telescopes and Instrumentation 2014: Optical, Infrared, and Millimeter Wave*, ed. J. Oschmann, Jacobus M., M. Clampin, G. G. Fazio, & H. A. MacEwen, 914320

Strohmeier, W., Three New Bright Eclipsing Binaries. 1972, *Information Bulletin on Variable Stars*, **665**, 1

van der Walt, S., Colbert, S. C., & Varoquaux, G., The NumPy Array: A Structure for Efficient Numerical Computation. 2011, *Computing in Science Engineering*, **13**, 22, DOI: 10.1109/MCSE.2011.37

Van Rossum, G. & Drake, F. L. 2009, *Python 3 Reference Manual* (Scotts Valley, CA: CreateSpace)